Modeling and Optimization of Double-Clad Fiber Amplifiers Using Chaotic Propagation of the Pump

Philippe Leproux, Sébastien Février, Valérie Doya, P. Roy, D. Pagnoux

Optical Fiber Technology, **6**, 324–339 (2001)
doi:10.1006/ofte.2001.0361, available online at http://www.idealibrary.com on IDEAL®

Modeling and Optimization of Double-Clad Fiber Amplifiers Using Chaotic Propagation of the Pump

P. Leproux and S. Février

Institut de Recherche en Communications Optiques et Micro-ondes, UMR CNRS n° 6615, Equipe Optique Guidée et Intégrée, 123 Avenue Albert Thomas, 87060 Limoges Cedex, France
E-mail: leproux@ircom.unilim.fr

V. Doya

Laboratoire de Physique de la Matière Condensée, Parc Valrose, 06108 Nice Cedex 02, France

and

P. Roy and D. Pagnoux

Institut de Recherche en Communications Optiques et Micro-ondes, UMR CNRS n° 6615, Equipe Optique Guideé et Intégrée, 123 Avenue Albert Thomas, 87060 Limoges Cedex, France

Received November 1, 2000; revised May 17, 2001

A complete theoretical study of double-clad fiber amplifiers is proposed. The notion of chaotic propagation is taken into account in order to improve the pumping process. In addition, a space–time algorithm is used to optimize the distribution of rare-earth dopant in the double-clad fiber. Finally, computed gain curves versus wavelength show attractive results for wavelength multiplexing applications.

Key Words: double-clad fiber, chaotic behavior, power amplifier

INTRODUCTION

In the past few years, double-clad fiber (DCF) amplifiers have made great strides in the optical power amplification field. Performances have been improved first

1068-5200/00 $35.00

thanks to new pumping technologies: end pumping [1] has been progressively replaced by side pumping [2–4], making it possible to leave the DCF ends free for fiber splicing. Moreover, the use of large area emitting laser diodes makes it possible to launch very high pump power, typically from a few to several tens of watts [5, 6]. High-level saturated signal output power can thus be reached, but with a very reduced efficiency. This is mainly due to the fact that the shape of the cross section of the fiber and/or the transverse distribution of rare-earth ions are not optimized, leading to an inefficient absorption of the pump power.

In this paper, we first theoretically study and optimize the pump power absorption into rare-earth-doped DCFs. The study deals with the design of a realistic inner clad geometry, allowing the most efficient pump absorption, all along the fiber. To achieve this goal, we show that it is necessary to achieve a so-called "chaotic propagation" of the pump. Then the designed fiber is used in a power amplifier, whose parameters (pump power, length, etc.) are optimized, by means of a space–time algorithm. The case of a 980-nm-pumped Er-doped DCF amplifier, operating in the range of wavelengths 1520–1580 nm, is considered. The calculations take into account the transverse distribution of Er^{3+} ions. In particular, a doped disc and a doped ring are investigated. Finally, computed curves of the gain versus wavelength are presented and discussed.

INFLUENCE OF THE SHAPE OF THE INNER CLAD ON THE PUMP ABSORPTION

The DCF used for power amplification consists of a single-mode core in which the signal propagates, surrounded by a large multimode core, called "inner clad," in which the pump power is launched. A low index clad is set around this inner clad. A rare-earth-doped area is introduced into the fiber, in order to allow the amplification process. The efficiency of this amplification process depends on numerous parameters, among which are the overlap integral between the signal distribution and the doped area (Γ_s), and the overlap integral between the pump power distribution and the doped area (Γ_p). Over an elementary length of propagation dz, the higher Γ_s and Γ_p are, the more efficient the amplification can be. Because of the single-mode propagation of the signal, Γ_s remains constant all along the fiber. Γ_s mainly depends on the location and on the extent of the doped area. The inner clad, which acts as a multimode core, has usually large dimensions and numerical aperture (NA), and consequently it guides a great number of modes. Each mode m_i takes part with the pumping process, the importance of this participation being proportional to the overlap integral γ_{m_i} between the mode field distribution and the rare-earth-doped section. Due to the differential mode absorption all along the fiber, the modal population may change with the distance z from the input end of the fiber, and consequently Γ_p may also depend on z. In order to increase the saturated signal output power and the efficiency of the amplifier, it is necessary to improve the pump power absorption by the rare-earth ions, all along the DCF [7]. Like this, some works have shown that offset doped core DCFs [8] could be suitable, despite technological manufacturing difficulties. In fact, to ensure that most

of the pumping energy can be absorbed, each mode must have some energy in the doped area. This desired feature can be obtained not by shifting the doped core, but by studying the shape of the inner clad cross section. As demonstrated in the next section, this better pump power absorption can be achieved in so-called "chaotic" DCFs.

CHAOTIC OR REGULAR PROPAGATION BEHAVIOR VERSUS THE CROSS SECTION OF THE CORE

Let us consider an optical step-index fiber, with a guiding core having an invariable cross section in the z-axis direction of propagation. Assuming that the transverse dimensions of this core are large compared to the wavelength, the ray optics approach can be used to describe the propagation of light in it. Using geometrical considerations, the cross section of the core can be seen as a two-dimension billiard, whose geometry governs the ray trajectory.

An incident ray launched into this billiard is submitted to successive reflections at the boundaries. In some cases, the ray trajectory is characterized by one of the two following properties:

(a) It is located in a certain region of the billiard (case of the circular fiber).
(b) It exhibits only few possible directions of propagation in the plane of the cross section (two directions in the case of the rectangular fiber).

The ray propagation in such a fiber is said to be regular.

Let us now discuss in more detail the cases of a circular core and of a rectangular one. In a conventional fiber, whose core is a circular billiard, the ray trajectory is regular (Fig. 1a). In particular, the distance d of the rays from the axis is always higher than a minimum value $r_{\min}$, depending on the angle α defined as the angle between the projection of the ray on the cross section and the tangent to the boundary of the core at the reflection point. The circle of radius $r_{\min}$ is called a "caustic." The value of $r_{\min}$ is null only for meridian rays associated to $\alpha = 90^\circ$. A break in the circular symmetry, for example, due to a straight cut in the core (D-shape), induces a complex ray trajectory (Fig. 1b). In such a billiard, except for meridian rays, any trajectory tends to explore the whole domain for a long length of propagation, without building regular structures such as caustics.

In the same way, a change from a regular to a nonregular behavior can also be observed when inducing a break into a rectangular fiber core: while one ray has only two directions of propagation in the rectangular billiard (Fig. 1c), it presents henceforth a lot of directions of propagation in the truncated rectangular billiard (Fig. 1d).

On can see that the cuts made on the circular and rectangular billiards induce a complex evolution of the rays, which propagate in many possible directions and over the whole area of the billiard. These are the characteristics of the so-called "chaotic" dynamic of rays. In other words, one of the main properties of a chaotic system is the ergodicity of the dynamic of rays [9, 10].

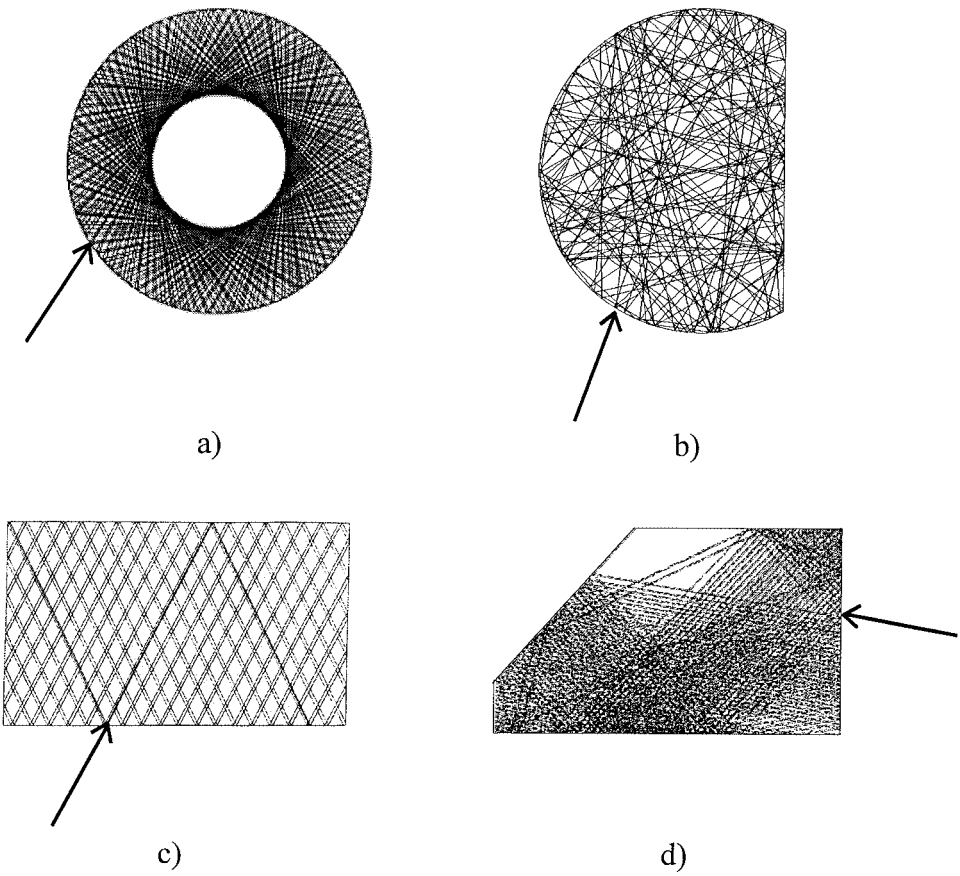

FIG. 1. Projection of a launched ray (direction and input point given by the arrow) in four different cross sections: (a) circular, (b) D-shape, (c) rectangular: regular propagation, and (d) rectangular with a break: chaotic behavior.

In terms of modes of propagation, nonchaotic fibers are characterized by the fact that the modes they guide exhibit a certain geometrical regularity in the field pattern, as is the case of circular fibers (LP modes) and rectangular fibers. Moreover, some modes of nonchaotic fibers can have their energy only located in some particular regions of the core. For example, Fig. 2a shows the $LP_{16,17}$ mode of a circular core fiber, for which no energy propagates near the center of the core.

In contrast, previous theoretical studies show that each high-order mode of a chaotic structure behaves as a diffuse field, so that its intensity distribution looks like an homogeneous speckle pattern distributed over the whole area of the core. This is illustrated in Fig. 2b, with a typical mode of a D-shape core fiber, computed by means of a collocation numerical method [11]. In a chaotic propagation structure having a cross section area S_T, for each high-order mode carrying the energy E, the part of this energy located in a region with the area S_R is approximately equal to $\frac{S_R}{S_T}E$, whatever the location of the considered region.

One can experimentally retrieve these regularities or irregularities by observing near-field patterns at the output end of different fibers. A circular core fiber and a

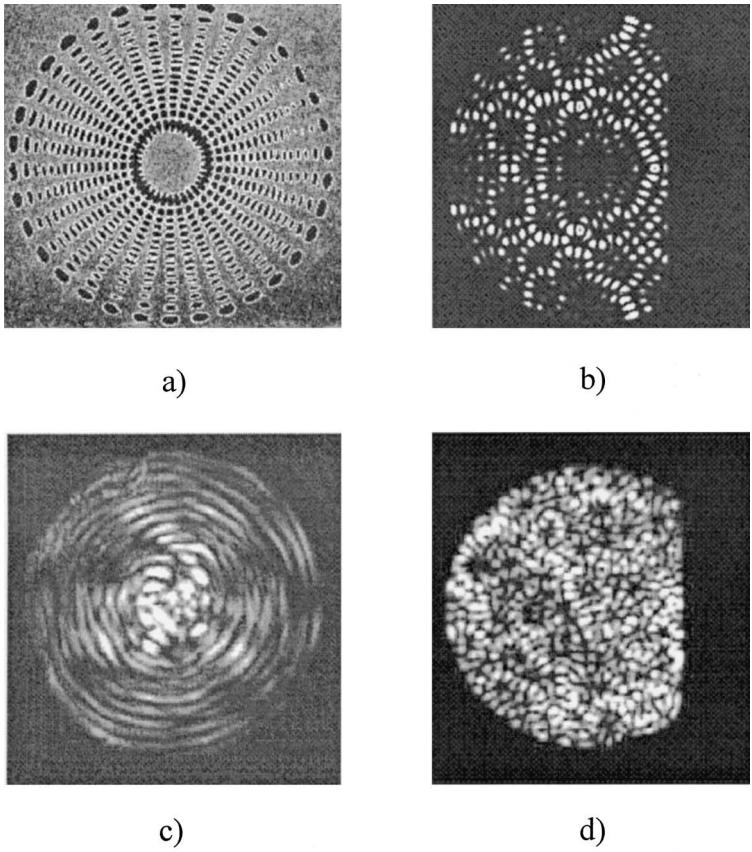

FIG. 2. Computed high-order mode field patterns in a circular (a) and a D-shape (b) step index core. Experimental speckle observed at the output of a circular (c) and a D-shape (d) step index core (excitation: centered *z*-directed laser beam focused on the input).

D-shape core one have been excited by a centered *z*-directed laser beam focused on their input end. In the case of the circular core fiber, a circular symmetry appears, with a higher energy density in the center (Fig. 2c), whereas a uniform speckle figure can be seen for the D-shape core fiber with the same conditions of excitation (Fig. 2d).

Let us now explain how chaotic propagation into DCFs can usefully be applied to power amplification.

QUANTITATIVE STUDY OF THE PUMP ABSORPTION BY MEANS OF THE BPM

The aim is now to quantitatively optimize the pump absorption into DCFs, by defining the most convenient shape of the inner clad cross section. We consider the case of Er-doped DCFs pumped at 980 nm, and operating at 1550 nm. Seven different inner clad cross section shapes, shown in Fig. 3, are considered. Some of

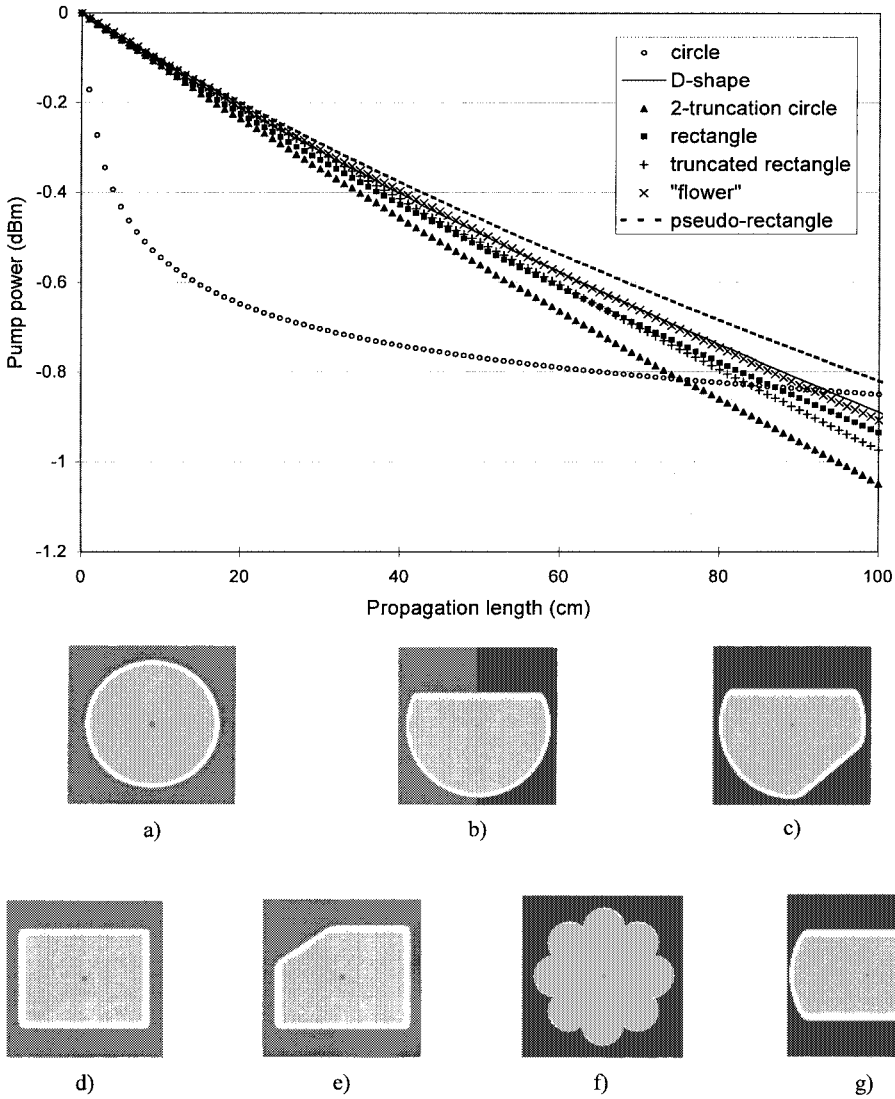

FIG. 3. Longitudinal evolution of the pump power for different inner clad shapes: (a) circle, (b) D-shape, (c) 2-truncation circle, (d) rectangle, (e) truncated rectangle, (f) "flower", and (g) pseudo-rectangle (excitation: 15-μm-shifted z-directed Gaussian beam).

them, such as those shown in Figs. 3a, 3d, and 3f, have already been presented in the literature. The seven fibers studied are assumed to have the same single-mode Er-doped core with a 6-μm diameter, a numerical aperture $NA_1 = 0.13$, and an Er concentration leading to a potential global attenuation of about 1 dB/m at 980 nm into the inner clad. For each fiber, the inner clad area in 15,000 μm^2 with a numerical aperture $NA_2 = 0.38$.

The algorithm implemented for the calculations of the pump absorption along the z-axis makes use of a 3-dimensional fast Fourier transform beam propagation method [12]. The 1-dB/m absorption in the inner clad is modeled by means of

a negative imaginary index. To couple the 980-nm pump energy into almost all the inner clad modes, the excitation is realized by a thin 15-μm-shifted z-directed Gaussian beam. The launched pump power is supposed to be equal to 0 dBm.

$P_p(z)$ is the longitudinal evolution of the pump power, expressed in dBm into the inner clad. It is plotted in Fig. 3 for a 1-m length of the seven DCFs considered.

In the case of the circular fiber (Fig. 3a), the decrease of the pump power is very strong over the very first centimeters of propagation, corresponding to the absorption of the low-order modes, whose overlap integral with the doped section is high. After a few centimeters of propagation, the remaining power is carried by high-order modes, which play a negligible part in the pumping process as they have very little or no energy in the central core. For that reason, the absorption of the pump falls under a very low value after about 50 cm of propagation, inducing a reduced population inversion and consequently a decrease of the local signal gain, or even a reabsorption of the signal, when the DFC is used into an amplifier.

The six other fibers exhibit a a significantly different absorption curve along the z-axis. The slope of the pump power curve in the very first centimeters is sensibly lower than for the circular fiber, but it remains much more regular all along the modeled length of fiber. Thus, beyond about 1 m, the rate of absorbed pump power becomes sensibly higher in these fibers than in the circular one. We have numerically verified that, over a longer piece of fiber, the more linear the decrease is, the higher the rate of absorbed pump power is, and hence the higher the signal gain can be. This optimum case corresponds to an homogeneous absorption of the pump all along the fiber. It can be obtained provided that the values of γ_{m_i} associated with each mode are close to each other. A modally nonselective absorption of the pump is then achieved, leading to quasi-constant attenuation of the pump power all along the fiber, and allowing an optimized pumping process. In other words, we can define an optimized cross section as a section for which each pump mode has approximately the same overlap integral with the doped section. According to the considerations of the previous section, this means that the propagation into an optimum inner clad cross section exhibits the most chaotic behavior.

In Fig. 3, we can see that the fiber with the 2-truncation circular section (Fig. 3c) exhibits the highest pump absorption over 1 m of fiber, and a very good linearity of $P_p(z)$. The reason is that the propagation into this fiber has the most chaotic behavior, as described in the previous section. This fiber, whose preform is easy to manufacture, appears to be the best one for achieving an efficient 1550-nm power amplifier.

CALCULATION OF THE GAIN OF A DCF AMPLIFIER, VERSUS THE INNER CLAD SHAPE OF THE FIBER

Let us now model amplifiers made with different DCFs of the previous paragraph, in order to evaluate the influence of the inner clad shape on the attainable performances.

The software used to model amplifiers has been developed in our laboratory. It is classically based on the resolution of the rate equations [13], taking into account the amplified spontaneous emission (S_{ASE}), together with the signal (P_s) and pump (P_p) powers [14]. The pump and signal overlap integrals (Γ_p and Γ_s) with the rare-earth-doped section are first calculated. Then the space–time evolution of the different above-mentioned powers is computed, taking into consideration the emission and absorption cross sections, the length of the fiber, and the rare-earth dopant concentration.

In particular, the space–time evolution of the population concentration in the excited state $N_2(z, t)$ can be deduced from the equation

$$\frac{dN_2(z,t)}{dt} = \frac{\sigma_a(\nu_p)}{h\nu_p} P_p(z,t) + W_{sa} N_1(z,t) - \left(W_{se} + \frac{1}{\tau_f}\right) N_2(z,t), \tag{1}$$

where $\sigma_a(\nu_p)$ is the pump absorption cross section, h is the constant of Planck, ν_p is the pump frequency, W_{sa} and W_{se} are respectively the signal absorption and emission rates, $N_1(z, t)$ is the population concentration in the ground state, and τ_f is the lifetime of the excited state.

W_{sa} and W_{se} can be calculated from P_s and S_{ASE} by

$$W_{se} = \left[\frac{\sigma_e(\nu_s)}{h\nu_s} P_s(z) + \int_0^\infty \frac{\sigma_e(\nu)}{h\nu} S_{ASE}(\nu, z) d\nu \right] \cdot \Gamma_s \tag{2}$$

$$W_{sa} = \left[\frac{\sigma_a(\nu_s)}{h\nu_s} P_s(z) + \int_0^\infty \frac{\sigma_a(\nu)}{h\nu} S_{ASE}(\nu, z) d\nu \right] \cdot \Gamma_s \tag{3}$$

with $\sigma_e(\nu_s)$ and $\sigma_a(\nu_s)$ being the signal emission and absorption cross sections, and ν_s the signal frequency.

We have studied three amplifiers, including respectively the circular, rectangular, and 2-truncation DCFs, whose opto-geometrical parameters are the same as above (single-mode core: diameter = 6 μm, $NA_1 = 0.13$, cut-off wavelength ≈ 1 μm; inner clad: area = 15,000 μm^2, $NA_2 = 0.38$). The background losses have been neglected, considering their low values into such DCFs (about 1 dB/km at 980 nm and less than 0.5 dB/km around 1550 nm) together with the short lengths of the studied amplifiers [13]. The computations have been realized at two different wavelengths (1530 and 1560 nm) for a −10-dBm 0.25-nm linewidth input signal. In each case, the pump power is 3 W with a spectral width of 2 nm. The computed results are presented in Fig. 4: we have plotted the evolution of the gain in decibels as a function of the fiber length, for each type of fiber, at 1530 nm (Fig. 4a) and 1560 nm (Fig. 4b). In the case of the circular DCF, the gain obtained for the optimal length of fiber (40 cm) barely reaches 2 dB at 1530 nm. As for the rectangular and 2-truncation DCFs, the maximum gain is respectively 5 and 17 dB, for respective optimal lengths 2 and 13 m, at 1530 nm. The performance discrepancies between these three fibers are directly related to the longitudinal evolution of the pump power shown above. Indeed, in the 2-truncation DCF, the reabsorption of the signal appears after a greater length of propagation than in the circular DCF, and is noticeably less important.

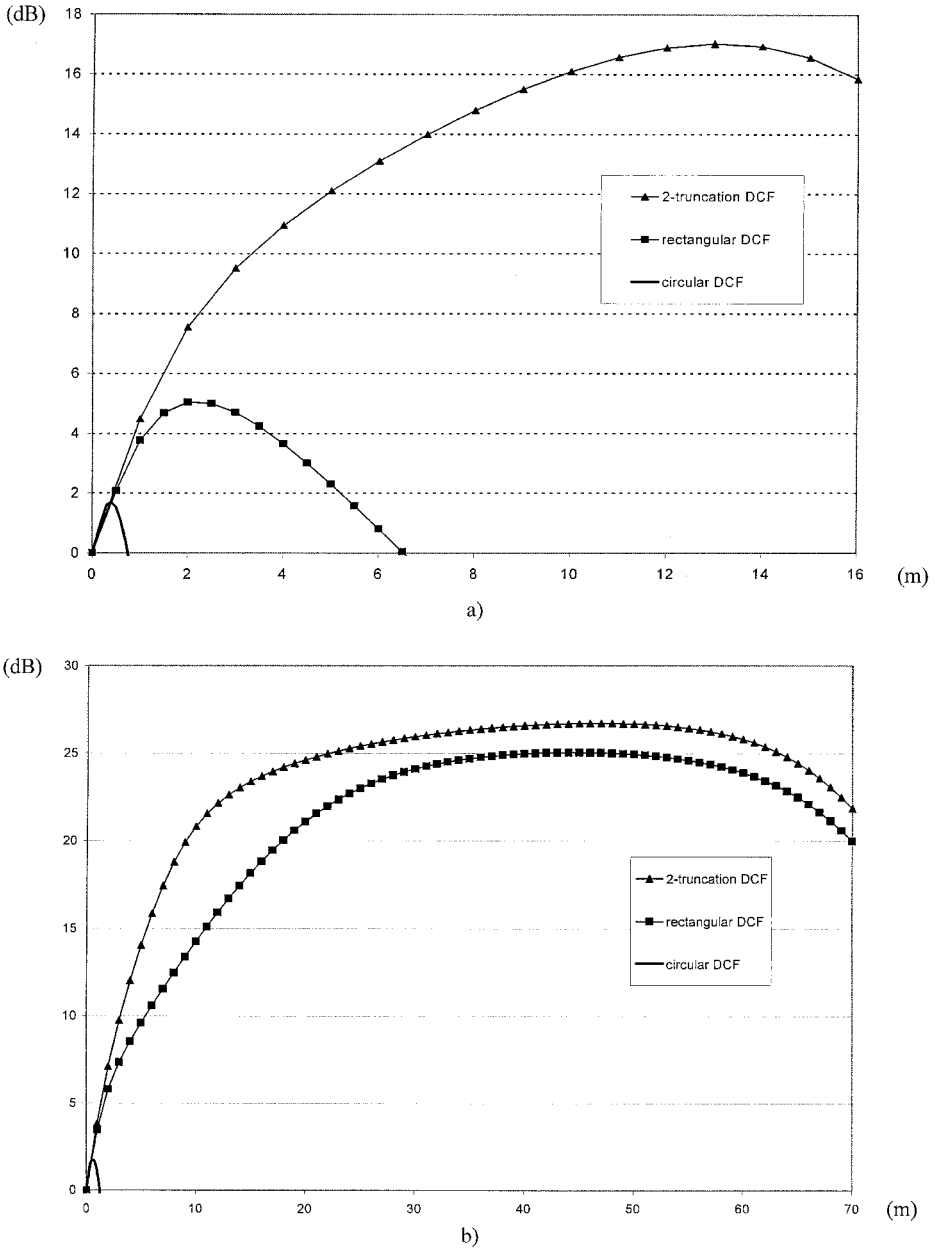

FIG. 4. Evolution of the gain as a function of the fiber length in three DCF amplifiers; pump power = 3 W; −10-dBm input signal power at (a) 1530 nm and (b) 1560 nm.

At 1560 nm, the circular DCF remains somewhat inefficient with a gain of less than 2 dB with a 0.6-m-long fiber. In contrast, the results obtained in the case of the rectangular DCF (25 dB of gain with a 45-m fiber) are close to those achieved with the 2-truncation one (27 dB of gain with a 47-m fiber). This is due to the fact that the gain at 1560 nm is obtained thanks to a near-4-level operation, for which the signal reabsorption remains very weak [13].

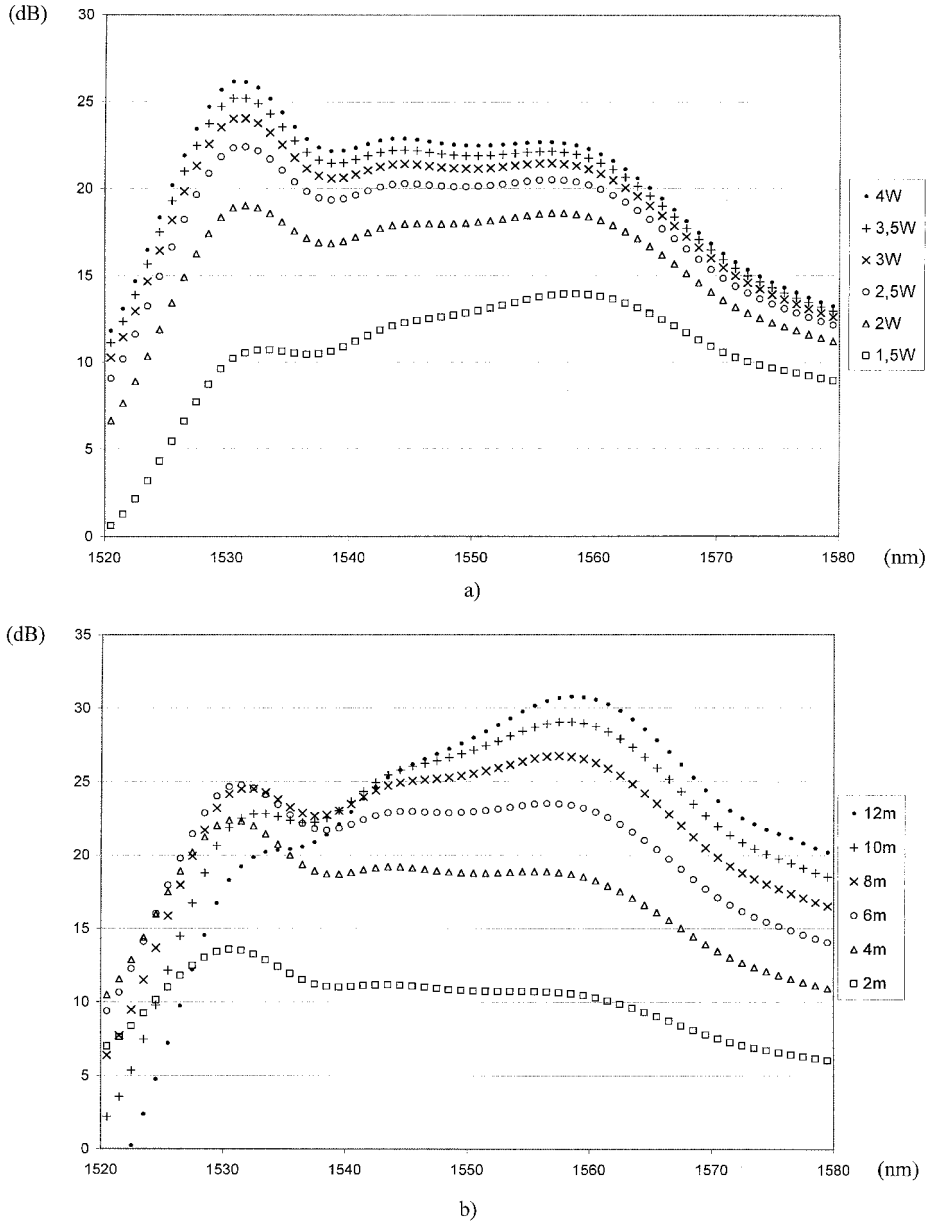

FIG. 5. Evolution of the gain as a function of the wavelength for a 2-truncation core-doped DCF; −10-dBm total input signal power equally distributed over 60 channels: (a) Fiber length = 5 m, pump power as a parameter and (b) Pump power = 3 W, fiber length as a parameter.

MODELING AND OPTIMIZATION OF A DOUBLE-CLAD 2-TRUNCATION CIRCULAR FIBER AMPLIFIER

The study applies now to a power amplifier including the 2-truncation circular DCF. The main assumption is that the pump energy distribution over the cross section of the inner clad remains uniform all along the z-axis, thanks to the chaotic

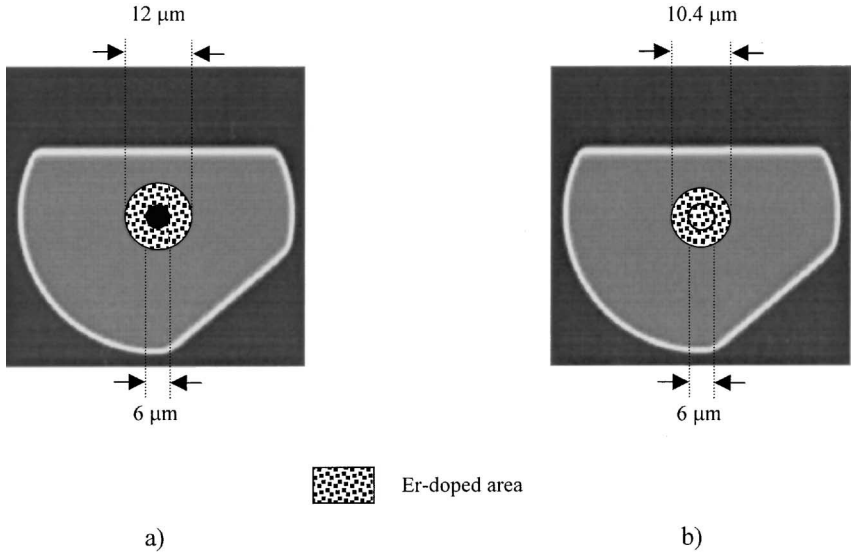

FIG. 6. Distribution of the rare-earth in the studied (a) ring-doped and (b) disc-doped DCF. The doped area is the same in both cases. The signal power distribution is as described in the legend to Fig. 5.

propagation of the light into the structure. The overlap integral between the pump (area $= S_T$) and the rare-earth-doped zone (area $= S_D$) is then assumed to remain equal to $\Gamma_P = \frac{S_D}{S_T}$ all along the z-axis.

In the following calculations, a 980-nm-pumped Er-doped power amplifier is considered. The single-mode core has a 6-μm diameter, with a numerical aperture $NA_1 = 0.13$. The inner clad has an area $S_T = 10{,}000\ \mu m^2$ and a numerical aperture $NA_2 = 0.38$. The Er concentration is uniformly equal to 1000 ppm over the doped area, whose location can be considered as a parameter.

The numerical simulations have been performed considering that the amplifier is used in a wavelength multiplexing transmission system. The -10-dBm signal input power is equally distributed over a set of 60 regularly spaced calculation channels, from 1520 to 1580 nm. Each signal linewidth is 0.25 nm. The results discussed below deal with the gain value in decibels, for each channel.

First, the Er-doped region is supposed to exactly coincide with the single-mode core. The evolution of the channel gain as a function of the wavelength is plotted in Fig. 5, for different pump power values and for different lengths of fiber. The resulting set of curves is in good agreement with the following theoretical predictions:

(a) For a given length of fiber (5 m), when the pump power is increased, the gain particularly increases around 1530 nm, the 3-level operation being favored thanks to an important population inversion (Fig. 5a).

(b) With a 3-W pump power, as the length of fiber is increased, the gain peak at 1530 nm falls because of the reabsorption. The latter leads to the excitation of Er^{3+} ions, subsequently able to amplify signals at longer wavelengths thanks to a 4-level operation, especially around 1560 nm. This is the reason why a maximum gain appears at 1560 nm (Fig. 5b).

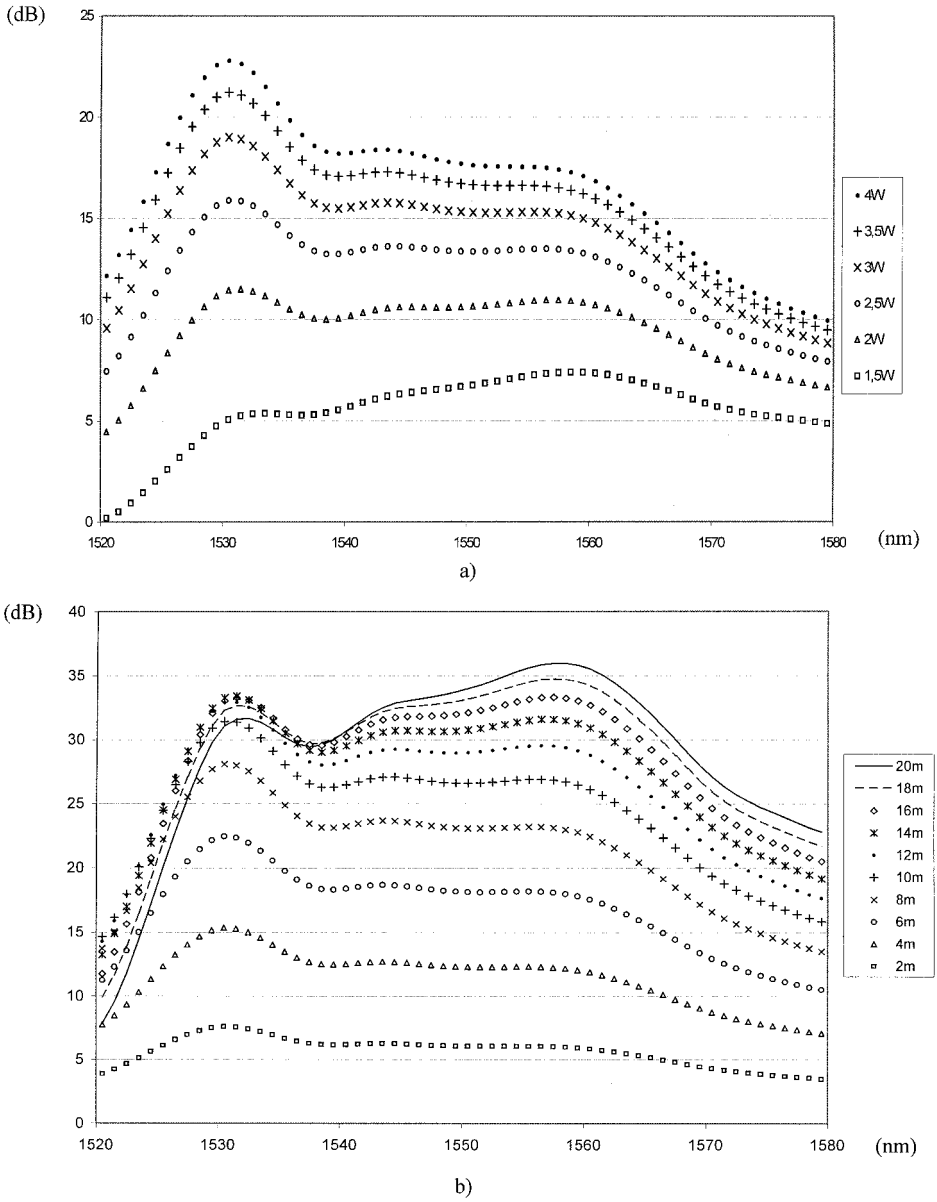

FIG. 7. Evolution of the gain as a function of the wavelength for the ring-doped DCF of Fig. 6a; same signal power distribution as described in the legend to Fig. 5: (a) Fiber length = 5 m, pump power as a parameter, and (b) pump power = 3 W, fiber length as a parameter.

One can notice that experimental results have been already reported concerning an Yb-free EDFA (Er-doped fiber amplifier) with output power performances higher than in the present work [15]. However, these published results are obtained with an amplifier having parameters sensibly different from those of our model. In particular, the ratio signal/pump core areas in the experiments is about 10 times higher than that of our calculations. Moreover, we consider a significantly larger

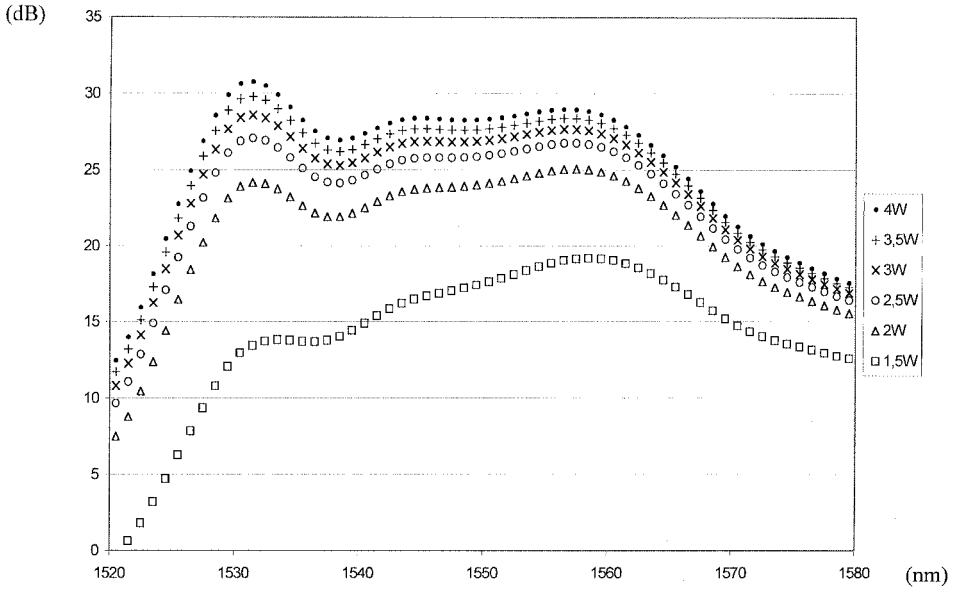

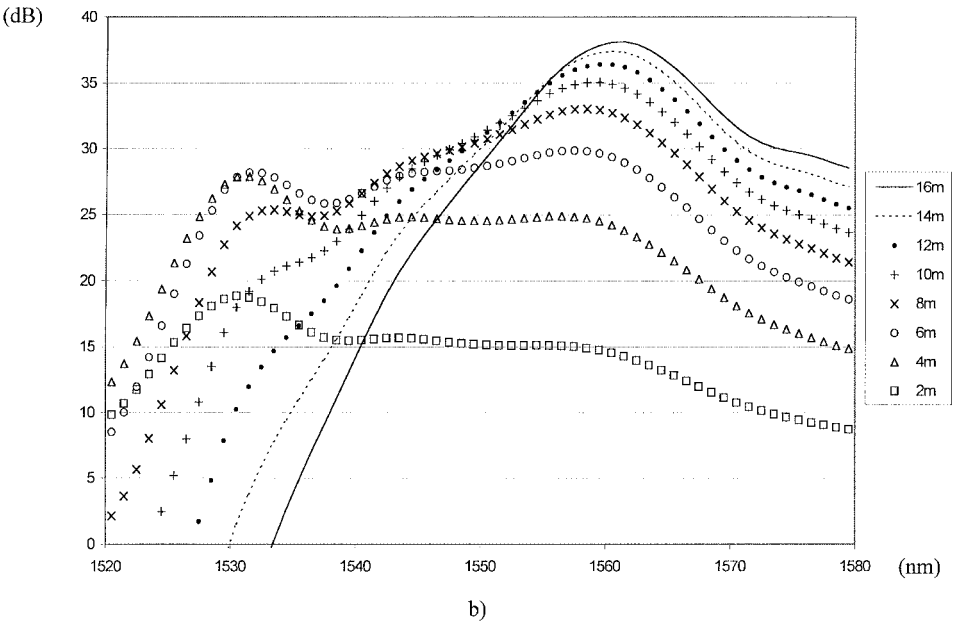

FIG. 8. Evolution of the gain as a function of the wavelength for a disc-doped DCF of Fig. 6b; same signal power distribution as described in the legend to Fig. 5: (a) Fiber length = 5 m, pump power as a parameter and (b) pump power = 3 W, fiber length as a parameter.

spectral band. That is why no direct quantitative comparison can be made between the two studies.

The software has also been used in order to optimize the location of the Er-doped zone, in the 2-truncation circular DCF. Two different types of distributions are considered: a centered disc somewhat larger than the single-mode core and a ring

[16, 17] set around the single-mode core (Fig. 6). For each kind of distribution, the dimensions of the Er-doped zone have been optimized in order to obtain a minimum gain of about 30 dB over the widest possible range of wavelengths, for a 3-W pump power. According to this criterion, the optimal ring-doped DCF provides better results than the optimal disc-doped DCF. In the following, the considered fibers are this optimal ring-doped DCF and a disc-doped DCF of the same Er-doped area as the optimal ring.

In the optimal ring-doped DCF, the ring is set side by side with the single-mode core and lies up to a radius of 6 μm (Fig 6a). Figure 7a shows that the peak at 1530 nm is typically accentuated when the fiber is better pumped. A more interesting behavior can be found in Fig. 7b: when the fiber length increases, for a given pump power value, both peaks (1530 and 1560 nm) become more pronounced. In other words, there is no fall in the 3-level operation, as was the case for the core-doped DCF. In fact, ring doping reduces the overlap integral Γ_S between the doped zone and the signal field, while not reducing the overlap factor Γ_P. The signal can thus be gradually amplified all along the fiber by limiting the reabsorption at 1530 nm. The channel gain curves can also be flatter than those obtained with a core-doped DCF. For instance, with a 16-m-long fiber and a 3-W pump power, one can obtain a minimum gain of almost 30 dB over a range of 35 nm (from 1530 to 1565 nm) with a flatness of ± 2 dB. The considered disc-doped DCF, whose Er-doped zone has the same area as that of the ring (disc radius = 5.2 μm), is shown in Fig. 6b. The two sets of channel gain curves (Figs. 8a and 8b) have been computed under the same conditions as previously. One distinctly can see that the behavior is comparable to that of the core-doped DCF, with a strong change from 3- to 4-level operation when the pumping decreases or when the fiber length increases. For example, with a 16-m-long fiber with a 3-W pump power, the gain around 1560 nm reaches 37 dB, whereas no gain can be obtained at 1530 nm. Moreover, we note that for short fiber lengths (for example, 5 m), the gain values obtained with disc doping (Fig. 8a) are higher than those obtained with ring doping (Fig. 7a).

Figure 9 shows the comparison of two amplifiers, that realized with a 12-m long ring-doped DCF, the other with a 4-m long disc-doped DCF, both amplifiers being pumped with 3 W at 980 nm. These lengths are chosen in order to achieve, for each amplifier, the highest gain with a flattened curve after the 1530-nm peak. The best curve obtained with the core-doped DCF (6 m length) has been likewise added. Let us note that ring doping requires a longer DCF because of the progressive amplification described above, but generally speaking, it makes it possible to attain performances better, with regard to potential broad band gain, than those obtained with core-doped or disc-doped DCFs.

The results presented here concern an EDFA. That is enough to modify the cross-sections values versus wavelength so that the software can take into account other dopant ions.

CONCLUSION

A precise and above all complete modeling of DCF amplifiers has been achieved, taking into account the cross section of the inner clad of the fiber and the distribu-

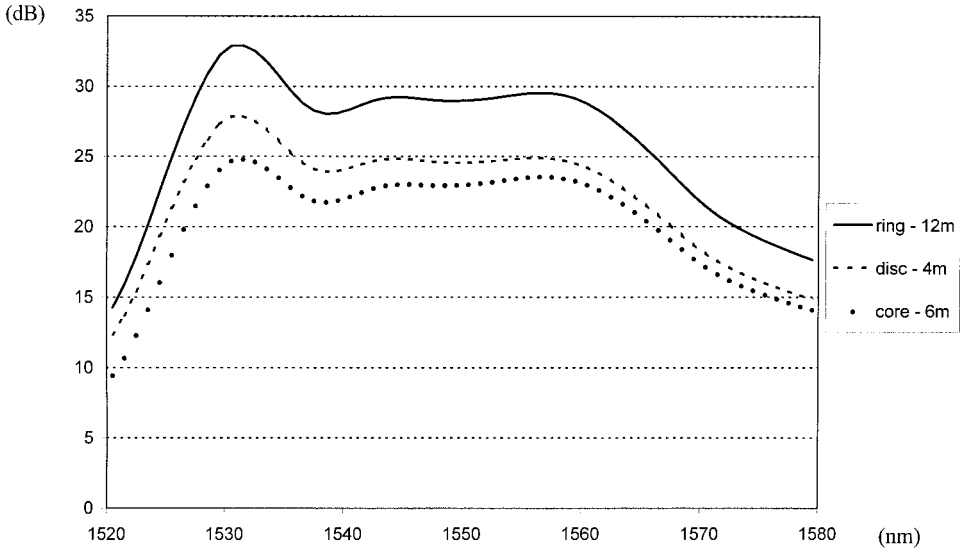

FIG. 9. Channel gain curves for three length-optimized DCFs with different distributions of the rare-earth: ring-doped DCF (12 m), core-doped DCF (6 m), disc-doped DCF (4 m); pump power = 3W; same signal power distribution as described in the length to Fig. 5.

tion of rare-earth ions. On the one hand, we showed that the wave chaos theory can be exploited so as to design optimal cross sections of the inner clad, allowing a highly efficient pumping operation. This represents an essential stage toward the optimization of an amplifier. On the other hand, the rare-earth dopant distribution has a strong influence on the shape of gain curves obtained with regard to wavelength. Different cases have been studied. Ring doping gives attractive characteristics, in terms of level and flatness of the gain, for EDFAs used in WDM applications. For example, a gain value of 30 dB over a 35-nm bandwidth is attainable with a flatness of ± 2 dB, in a 16-m-long Er-ring-doped DCF pumped at 980 nm with 3 W, for -10-dBm input signals.

ACKNOWLEDGMENTS

The authors are grateful to F. Mortessagne and O. Legrand from LPMC Nice for helpful discussions.

REFERENCES

1. T. Miyazaki, K. Inagaki, Y. Karasawa, and M. Yoshida, "Nd-doped double-clad fiber amplifier at 1.06 μm," *J. Lightwave Technol.*, vol. 16, no. 4, 562 (1998).
2. Th. Weber, W. Lüthy, H. P. Weber, V. Neuman, H. Berthou, and G. Kotrotsios, "A longitudinal and side-pumped single transverse mode double-clad fiber laser with a special silicone coating," *Opt. Commun.*, vol. 115, 99 (1995).
3. D. J. Ripin and L. Goldberg, "High efficiency side-coupling of light into optical fibres using imbedded v-grooves," *Electron. Lett.*, vol. 31, no. 25, 2204 (1995).
4. J. P. Koplow, L. Goldberg, and D. A. V. Kliner, "Compact 1-W Yb-doped double-cladding fiber amplifier using v-groove side-pumping," *IEEE Photon. Technol. Lett.*, vol. 10, no. 6, 793 (1998).

5. V. Dominic, S. MacCormack, R. Waarts, S. Sanders, S. Bicknese, R. Dohle, E. Wolak, P. S. Yeh, and E. Zucker, "110W fiber laser," in *Proc. of Conference on Lasers and Electro-Optics, Baltimore, MD*, Post-deadline paper CPD26, 1999.
6. A. B. Grudinin, J. Nilsson, and P. W. Turner, "New generation of cladding pumped fibre lasers and amplifiers," in *Proc. of Conference on Lasers and Electro-Optics, Nice, France*, Invited paper CWA3, 2000.
7. E. Desurvire, J. L. Zyskind, and C. Randy Giles, "Design optimization for efficient Erbium-doped fiber amplifiers," *J. Lightwave Technol.*, vol. 8, no. 11, 1730 (1990).
8. A. Liu and K. Ueda, "The absorption characteristics of circular, offset, and rectangular double-clad fibers," *Opt. Commun.*, vol. 132, 511 (1996).
9. F. Mortessagne, O. Legrand, and D. Sornette, "Role of the absorption distribution and generalization of exponential reverberation law in chaotic rooms," *J. Acoust. Soc. Am.*, vol. 94, 154 (1993).
10. V. Doya, F. Mortessagne, O. Legrand, E. Picholle, Ch. Miniatura, and R. Kaiser, "Contrôle de l'ordre et du désordre spatial dans une fibre optique chaotique," in *Proc. of Journées Nationales d'Optique Guidée, France*, pp. 295–297, 1998.
11. E. J. Heller, "Wave packet dynamics and quantum chaology," in *Proc. of Summer School on Chaos and Quantum Physics*, NATO Org., Les Houches, France, 1989.
12. A. Tervonen, "Software tools for integrated optics design," *Proc. SPIE*, vol. 2997, 202 (1997).
13. E. Desurvire, *Erbium-doped Fiber Amplifiers*, Wiley–Interscience, New York, 1994.
14. B. Pedersen, A. Bjarklev, J. H. Povlsen, K. Dybdal, and C. C. Larsen, "The design of Erbium-doped fiber amplifiers," *J. Lightwave Technol.*, vol. 9, no. 9, 1105 (1991).
15. F. Leplingard, P. Bousselet, M. Bettiati, L. Gasca, L. Lorcy, A. Tardy, and D. Bayart, "High-power (+24 dBm) double-clad erbium-doped fibre amplifier for WDM applications in the C-band (1528 nm–1562 nm)," in *Proc. of Conference on Lasers and Electro-Optics, Nice, France*, Paper CFG3, 2000.
16. J. Nilsson, R. Paschotta, J. E. Caplen, and D. C. Hanna, "Yb^{3+}-ring-doped fiber for high-energy pulse amplification," *Opt. Lett.*, vol. 22, no. 14, 1092 (1997).
17. J. Nilsson, J. D. Minelly, R. Paschotta, A. C. Tropper, and D. C. Hanna, "Ring-doped cladding-pumped single-mode three-level fiber laser," *Opt. Lett.*, vol. 23, no. 5, 355 (1998).